Supporting Information

SI Materials and Methods

Bacterial strains, plasmids, and instruments. *E. coli* Top10, BL21 Gold (DE3), and BL21 Star were purchased from Invitrogen. *Pseudomonas putida* F1, *P. putida* ATCC 17633, and *P. putida* S12 were obtained from the American Type Culture Collection. *P. fluorescens* Pf-5, *P. aeruginosa* PAO-1, *P. aeruginosa* PA14, *P. syringae* pv. *syringae* B301D, *P. syringae* pv. *syringae* B728a, *P. syringae phaseolicola* NPS3121, and *P. putida* KT2442 were gifts from Prof. Christopher Walsh of Harvard Medical School. *Pseudomonas syringae* TLP2, *P. syringae* Cit7, and *P. syringae* pv. *tomato* DC3000 were gifts from Prof. Steven Lindow of UC Berkeley. *Shewanella* CN-32, MR1, MR4, MR7, SB-213, W3-18-1, and Awa3 were gifts from Prof. Adam Arkin of UC Berkeley. *P. aeruginosa* PA14 transposon insertion mutants were purchased from Massachusetts General Hospital (Boston, MA).

Media and chemicals were purchased from Difco, Sigma-Aldrich, and EMD Chemicals. Oligonucleotide primers were synthesized by Elim Biopharm, and PCR was performed with Phusion High-Fidelity PCR Master Mix (NEB). Cloning was performed using the Xa/LIC Cloning Kit (Novagen), Zero Blunt PCR Cloning Kit (Invitrogen), or restriction enzymes from NEB. Recombinant plasmid DNA was purified with a QIAprep kit (Qiagen). DNA sequencing was performed at Quintara Biosciences (Albany, CA). Site-directed mutagenesis was performed by using the QuikChange Site-Directed Mutagenesis Kit (Agilent). SDS-PAGE gels and nickel-nitrilotriacetic acid agarose (Ni-NTA) superflow resin were purchased from Biorad and Qiagen, respectively. Protein samples were concentrated using the 10 kDa cutoff Amicon Ultra-15 Centrifugal Filter Units (Millipore). DNA and protein concentrations were determined by a Nanodrop 1000 spectrophotometer (Thermo Scientific).

Typical GC-MS analysis was conducted on a Varian CP-3800 instrument equipped with a Varian 320-MS using a Varian factorFOUR capillary column (30 m, 0.25 mm, DF = 0.25). Carbon dioxide analysis was performed with a gastight syringe (Hamilton) and Agilent 5975C GCMS system equipped with Agilent Technologies J&W HP-PLOT Q column (30 m, 0.32 mm, 20.00 μm).

Bacterial growth and hydrocarbon analysis. *E. coli*, *P. aeruginosa* PAO1, and *P. aeruginosa* PA14 strains were grown in 5 mL of LB medium overnight at 37°C, while all the other *Pseudomonas* and *Shewanella* strains were grown at 30°C. For 1-undecene production, 50 μL of seed culture was used to inoculate 5 mL of LB medium. The culture was shaken in a sealed 20 mL headspace vial (Agilent certified) containing a stir bar at 30°C for 36 hr. For the feeding experiments, 200 μM of either [12-^{13}C]LA or [1-^{13}C]LA was added to the culture (Fig. S1). After incubation, an SPME fiber (30 μm polydimethylsiloxane, Supelco, Sigma-Aldrich Group, Bellefonte, PA) was manually inserted into the headspace vial and incubated at 25°C for 12.5 min. GC-MS analysis was conducted on a Varian CP-3800 instrument equipped with a Varian 320-MS. The analytes were desorbed from the fiber at 280°C in a splitless injector equipped with a 78.5 mm × 6.5 mm × 0.75 mm liner (Sigma), and developed on a Varian factorFOUR capillary column (30 m x 0.25 mm, DF = 0.25) using helium as the carrier gas (1 mL/min) and the following temperature gradient: initial 50°C for 3 min, ramped at 10°C/min to 130°C, ramped at 30°C/min to 300°C, and then held for 5 min. The mass spectrometer was operated in electron ionization mode with automatically tuned parameters; the acquired mass range was 15–250. The signals of the 1-alkenes were identified and quantified by comparison with authentic samples (MP Biomedicals), which were diluted in ethyl acetate, added to 5 mL of culture medium in a sealed headspace vial, and sampled by the same SPME-GCMS method as mentioned above. We assessed 1-undecene production by various bacteria strains including *P. fluorescens* Pf-5 (100 ng/mL), *P. aeruginosa* PAO1 (15 ng/mL), *P. aeruginosa* PA14 (10 ng/mL), *P. syringae* pv. *syringae* B301D (10 ng/mL), *P. syringae* pv. *syringae* B728a (100 ng/mL), *P. syringae* TLP2 (70 ng/mL), *P. syringae* Cit7 (100 ng/mL), *P. syringae phaseolicola* NPS3121 (10 ng/mL), *P. syringae* pv. *tomato* DC3000 (20 ng/mL), *P. putida* F1 (2 ng/mL), *P. putida* ATCC 17633 (2 ng/mL), *P. putida* KT2442 (1-2 ng/mL), *P. putida* S12 (1-2 ng/mL), *Shewanella* CN-32, MR1, MR4, MR7, SB-213, W3-18-1, Awa3, *E. coli* Top10, BL21 Gold (DE3), BL21 Star, and EPI300. 1-undecene was not detected in the fermentation cultures of *Shewanella* and *E. coli*.

Identification of the 1-undecene biosynthetic gene. Molecular biology procedures and DNA manipulations were carried out according to standard protocols. The fosmid genomic library of *P. fluorescens* Pf-5 was constructed using a pCC2Fos CopyControl library kit following the manufacturer's protocol (Epicentre Biotechnologies) (Fig. S2). The host used for library

construction was *E. coli* EPI300. 10 individual colonies were combined to inoculate 500 μL of LB with chloramphenicol (25 μg/mL) in each well of the 96 deepwell plates (Nunc), and 6 plates were generated from a library of ~6000 fosmids. To screen the library, 30 μL of seed culture from each tens-of-clones was used to inoculate 3 mL of LB with chloramphenicol (25 μg/mL) and CopyControl Fosmid Autoinduction Solution (Epicentre Biotechnologies), and the culture was shaken in a sealed 20-mL headspace vial containing a stir bar (Agilent certified) at 30°C for 36 hr. The headspace volatiles were sampled by the SPME GC-MS method mentioned above to screen for 1-undecene-producing cultures. Positive tens-of-clones were sub-cultured, and another round of screening was performed to identify single 1-undecene-producing clones. Three fosmids, 6F8, 6E2, and 4F3, were sequenced to reveal a 15-kb overlapping region.

The overlapping insertion region of 6F8 was digested with HindIII/XbaI and ligated into pCR-Blunt vector to give pZR52 (Fig. S2). After *E. coli* EPI300 (pZR52) was confirmed to produce 1-undecene, pZR52 was digested with BglII/HindIII or BglII/XbaI and ligated into pCR-Blunt to yield pZR56 or pZR57, respectively. pZR56 and pZR57 were subsequently introduced into *E. coli* TOP10 (Invitrogen) to examine 1-undecene production as mentioned above. As *E. coli* EPI300 (pZR57) but not *E. coli* EPI300 (pZR56) produced 1-undecene, pZR57 was further digested with SmaI/XbaI to give pZR59, which conferred 1-undecene production in *E. coli* TOP10 (pZR59). *undA* was PCR-amplified by using pZR60-F/R as primers (Table S1) and pZR59 as a template, and cloned into pET-30Xa-LIC under a T7 promoter to yield pZR60. All of the plasmid constructs were confirmed by DNA sequencing. pZR60 was introduced into *E. coli* BL21 Star, which was grown at 37°C in 30 mL of LB medium supplemented with 50 μg/mL kanamycin. Once the OD_{600} reached 0.6, a 3 mL aliquot was transferred into the headspace vial and induced with 0.1 mM of isopropyl-β-D-thiogalactopyranoside (IPTG) at 30°C for 24 hr. 1-Undecene production was detected by using the SPME-GCMS method. *PFL_4320* was also overexpressed in *E. coli* BL21 Star, but failed to enable the 1-undecene production.

Small-scale 1-alkene production in *E. coli.* *PSPTO_1738* (*P. syringae pv. tomato* DC3000), *PA14_53120* (*P. aeruginosa* PA14), and *Pput_3952* (*P. putida* F1) were PCR-amplified by using pZR80-F/R, pZR95-F/R, and pZR97-F/R as primers (Table S1) and their corresponding genomic DNA as templates, and cloned into pET-30Xa-LIC under a T7 promoter to yield pZR80, pZR95, and pZR97. All of the expression constructs were confirmed by DNA sequencing and introduced

into *E. coli* BL21 Star for 1-undecene production. A starter *E. coli* culture was grown overnight in 5 mL of LB medium at 37 °C and 250 rpm, and 0.3 mL was used to inoculate 30 mL of LB medium supplemented with 0.5% glycerol and 50 μg/mL kanamycin, which was shaken at 37 °C until the OD_{600} reached 0.6. A 3 mL aliquot was transferred to a headspace vial and induced with 0.1 mM IPTG at 30°C for 24 hr before SPME-GCMS analysis.

Overexpression and purification of UndA. To overexpress *undA* for enzymatic analysis, *E. coli* BL21 Gold (DE3, pZR60) was grown in 1 L of LB medium with 50 μg/mL kanamycin until OD_{600} 0.6, harvested, and lysed as mentioned below. The insoluble fraction was removed by centrifugation, and the soluble proteins were incubated with 1 mL of Ni-NTA beads (Qiagen) on a nutator at 4°C for 1 hr. The proteins were then loaded onto a gravity flow column, washed with washing buffer (50 mM imidazole, 20 mM Tris, 300 mM NaCl, pH 8.5), and eluted with eluting buffer (250 mM imidazole, 20 mM Tris, 300 mM NaCl, pH 8.5). Purified proteins were exchanged into 20 mM Tris (pH 8.5) and 300 mM NaCl using Amicon Centrifugal Filter Units, flash frozen in liquid nitrogen, and preserved at -80°C.

To overexpress *undA* for protein X-ray crystallization, the gene was PCR-amplified by using pZR60-F_HRV3C/pZR60-R as primers (Table S1) and pZR59 as a template, and cloned into pET-30Xa-LIC under a T7 promoter to yield pZR60_HRV3C. *E. coli* BL21 Gold (DE3, pZR60_HRV3c) was grown in 1 L of Terrific Broth medium (24 g/L yeast extract, 12 g/L tryptone, and 10 g/L NaCl, pH 7.4) containing 6 mL of glycerol and 50 μg/mL kanamycin to an OD_{600} of 1.0-1.2. The culture was cooled on ice for 10 min, induced with 0.1 mM of IPTG, and grown at 180 rpm and 25°C for 12 hr. The cells were spun down and resuspended in 70 mL of lysis buffer (50 mM Tris, pH 8.5, 300 mM NaCl, 50 mM imidazole, and Sigma® protease inhibitor cocktail), and lysed on ice by homogenization using a Emulsiflex-C3 homogenizer. The soluble proteins were collected by centrifugation at 20,000 g and 4°C for 1 hr, and the supernatant was loaded onto a 5-mL Ni-affinity HisTrap HP column (GE Healthcare). The recombinant UndA was eluted with a gradient of 50-300 mM imidazole in 20 mM Tris (pH 8.5) and 300 mM NaCl, and the imidazole was thoroughly removed by passing the eluent through a Hiprep 26/10 desalting column (GE Healthcare). 100 mg of His-tagged UndA was digested with 0.5 mg of human rhinovirus 3C proteinase (QB3 Macrolab, UC Berkeley) at 4°C for 20 hr. The digested mixture was loaded onto a 5-mL Ni-affinity HisTrap HP column (GE Healthcare). The

flow-through was collected, added with 0.85 M ammonium sulfate, and loaded onto a Resource PHE column (GE Healthcare) equilibrated with 1 M ammonium sulfate and 20 mM Tris pH 8.0 at room temperature. Bound UndA was eluted with a gradient of 850-0 mM ammonium sulfate and 20 mM Tris over 50 column volumes, and concentrated in 10 mM Tris (pH 8.5), 100 mM NaCl, and 200 mM ammonium sulfate with Amicon® Ultra filters for crystallization.

Reconstitution of holo-UndA *in vitro*. The apo-UndA was rendered anoxic on a vacuum line by 5 cycles of evacuation and N_2 purge. To prevent reaction of the Fe(II) center with O_2, all subsequent manipulations to obtain UndA-Fe(II) were carried out anaerobically with stringently deoxygenated solutions. 1 mM of UndA was incubated with 1 mM of $(NH_4)_2Fe(SO_4)_2$ and 1 mM DTT for 30 min in the anaerobic chamber before desalting on the GE Disposable PD-10 columns equilibrated in 10 mM Tris (8.5), 100 mM NaCl, and 200 mM $(NH_4)_2SO_4$. The desalted enzyme solution was analyzed by ICP-MS (Perkin Elmer Optima 5300 DV), and the iron concentration was fitted to the calibration curve obtained using four standard solutions (Sigma-Aldrich) in the range 10-1000 μg/L. For *in vitro* enzymatic assays, the desalted UndA-Fe(II) was immediately used in the enzymatic reaction to achieve maximum activity.

Stoichiometry determination in single-turnover reactions and UndA activity toward selective substrates. To investigate 1-undecene formation and the O_2 consumption, 0.5 mL of reaction mixture contains 50 mM MES buffer (pH 6.2), 300 mM NaCl, 45 μM UndA-Fe(II), and 500 μM LA (25 mM stock solution of LA sodium salt was prepared in 2% tergitol; tergitol is not required for < 150 μM of LA). MES buffer (pH 6.2) was selected to reach slightly higher enzymatic activity than other buffers such as Bis-Tris (pH 6.0-7.0), Tris (pH 7.5-8.5), MOPS (pH 6.5-7.5), and HEPES (pH 6.8-8.0). The reaction was performed in a sealed headspace vial, initiated by adding UndA at room temperature and quenched by injecting equal volume of 5 M NaOH. 1-Undecene production was analyzed and quantified using the SPME-GCMS method. The correlations of total 1-undecene produced and enzyme used were further determined varying UndA concentrations (40-1000 μM), and similar single turnover reactions were obtained in all assays (~0.7-0.8 molecule of 1-undecene per molecule of UndA-Fe(II)). O_2 concentration was measured in a sealed reaction chamber (0.5 mL) with an integrated oxygen electrode unit (Oxygraph Plus System, Hansatech Instruments, UK) (Fig. S4). For the control group, LA was

omitted from the reaction mixture. To test the UndA activity toward various substrates, the reaction mixture is the same as described above except that the 500 μM of LA was substituted by 500 μM of alternative acids (Fig. 2 and S7-11).

H_2O_2 detection. For the detection of H_2O_2, the enzymatic reaction was conducted by using the oxygen electrode unit as mentioned above. After the concentration of O_2 reached equilibrium, 120 U/mL of catalase was added to the reaction chamber. We observed no rapid increase in the O_2 concentration, suggesting that no H_2O_2 was present in the reaction mixture. Alternatively, no obvious production of H_2O_2 was detected using Amplex® Red Hydrogen Peroxide/Peroxidase Assay Kit. 250 μL of reaction mixture contains 50 mM MES buffer (pH 6.2), 200 mM $(NH_4)_2SO_4$, 500 μM UndA-Fe(II), and 1 mM LA. The reaction mixture was subjected to centrifugation using Amicon® Ultra filters (3kD cutoff) and 50 μL of flowthrough was added to 50 μL of the Amplex® Red Hydrogen Peroxide working solution, incubated for an hour at room temperature in dark, and examined with excitation/emission maxima = 570/585 nm for fluorescence as instructed. The positive controls contain 50 mM MES buffer (pH 6.2), 200 mM $(NH_4)_2SO_4$, 500 μM $(NH_4)_2Fe(SO_4)_2$, 500 μM LA, and various amounts of standard H_2O_2 either provided by the same kit or Sigma. The positive controls showed this coupled assay had a sensitivity of 1 μM for H_2O_2 in the original reaction mixture of UndA.

Enzyme recycling experiments. To recycle the UndA, 1 mL of the oxygenated buffer solution (50 mM MES, pH 6.2, 100 mM NaCl) was mixed with 1 mL of an O_2-free solution containing 50 mM MES buffer (pH 6.2), 100 mM NaCl, 200 μM UndA, 1 mM $(NH_4)_2Fe(SO_4)_2$, 2 mM LA, so that the final mixture contains 50 mM MES buffer (pH 6.2), 100 mM NaCl, 100 μM UndA, 0.5 mM $(NH_4)_2Fe(SO_4)_2$, and 1 mM LA. This original reaction was quenched by adding 10-fold excess of EDTA to iron. The mixture was desalted on a GE Disposable PD-10 column and incubated at 4°C on a nutator for two hours to completely remove the residue 1-undecene in the solution. The recycled apo-UndA was concentrated by using Centrifugal Filter Units (Millipore) and subjected to a second enzymatic assay that contains 50 mM MES buffer (pH 6.2), 100 mM NaCl, 100 μM UndA, 0.5 mM $(NH_4)_2Fe(SO_4)_2$, and 1 mM LA. To initiate the reaction, 100 μL of the oxygenated buffer solution (50 mM MES, pH 6.2, 100 mM NaCl) was mixed with 100 μL of an O_2-free solution containing 50 mM MES buffer (pH 6.2), 100 mM NaCl, 200 μM UndA, 1

mM $(NH_4)_2Fe(SO_4)_2$, 2 mM LA. The control group was set up under similar conditions except that the original apo-UndA which had not been used for any enzymatic reactions was used. The experimental group containing recycled UndA produced 80% of the 1-undecene compared with the control group that contained the original UndA. When EDTA was omitted, the desalted recycled UndA failed to catalyze the reaction to produce 1-undecene.

Initial production rate determination. To determine the initial rates of 1-alkene production under the single turnover conditions, the O_2-saturated buffer solution (50 mM MES, pH 6.2, 100 mM NaCl) was mixed with an equal volume of an O_2-free solution containing 50 mM MES buffer (pH 6.2), 100 mM NaCl, 200 μM $(NH_4)_2Fe(SO_4)_2$, 0.2-20 μM UndA, and various concentrations of substrate (2-300 μM), so that the final mixture contains 50 mM MES buffer (pH 6.2), 100 mM NaCl, 0.1-10 μM UndA, 100 μM $(NH_4)_2Fe(SO_4)_2$, and various concentrations of substrate (1-150 μM) (Fig. S6-S8). The reactions were carried out in sealed GC vials and quenched by injecting 1 M NaOH at 2, 4, 6, 8, 10, 20, 30, 40, 50, 60 seconds. The productions of 1-alkenes were analyzed by SPME-GCMS analysis. The acquired 1-alkene production rates were plotted against fatty acid concentrations as shown in Fig. S6.

Reductive co-substrate screening. To survey the possible reductive co-substrates, the oxygenated buffer solution (50 mM MES, pH 6.2, 100 mM NaCl) was mixed with an equal volume of an O_2-free solution containing 50 mM MES buffer (pH 6.2), 100 mM NaCl, 200 μM UndA, 200 μM $(NH_4)_2Fe(SO_4)_2$, 2 mM LA, and 4 mM of the reductive co-substrate, so that the final mixture contains 50 mM MES buffer (pH 6.2), 100 mM NaCl, 100 μM UndA, 100 μM $(NH_4)_2Fe(SO_4)_2$, 1 mM LA, and 2 mM of the reductive co-substrate. The reaction was carried out in a sealed GC vial due to the semi-volatility of 1-undecene. For the chlorite dismutase coupled assay, 2 μM of chlorite dismutase (1) was included in the mixture, and 1 mM of sodium chlorite was injected through the septa four times every 20 min (Fig. S5). 2 mM of reductive co-substrate was added with the following exceptions: 40 μM FAD or FMN was coupled with 20 μM flavin reductase (AsuE2 (2)) and 2 mM NAD(P)H; 40 μM ferredoxin was coupled with 20 μM ferredoxin reductase and 2 mM NAD(P)H; 40 μM of pyrroloquinoline quinone was coupled with 2 mM of cysteine (3); and 40 μM phenazine methosulfate was coupled with 2 mM NADH (4).

Test of H_2O_2 as a possible substrate. To examine whether the H_2O_2/Fe^{3+} or the H_2O_2/Fe^{2+} system enables the UndA activity, we first performed the anaerobic enzymatic reactions in the glove box. The deoxygenated reaction mixture contains 50 mM MES buffer (pH 6.2), 100 mM NaCl, 100 μM UndA, 100 μM either $FeCl_3$ or $(NH_4)_2Fe(SO_4)_2$, 1 mM LA, and various amount of H_2O_2 (100, 200, 500, 1000, 5000 μM), and 1-undecene production was analyzed. The aerobic reaction was carried out under similar conditions except that the O_2 was provided by mixing with the equal volume of O_2-saturated buffer solution (50 mM MES, pH 6.2, 100 mM NaCl).

Production of CO_2. For the detection of CO_2**,** a 9.5 mL of reaction mixture contains 50 mM MES buffer (pH 6.2), 300 mM NaCl, 100 μM $(NH_4)_2Fe(SO_4)_2$, 1 mM ascorbic acid, 100 μM LA, and 10 μM UndA. The reaction was performed in a 10-ml sealed headspace vial (Agilent) and initiated by adding the enzyme. 100 μL of the headspace gas was acquired using a gastight syringe (Hamilton) and injected into Agilent 5975C GCMS system equipped with an Agilent Technologies J&W HP-PLOT Q column (30 m, 0.32 mm, 20.00 μm). Injector temperature was set at 120°C, and helium was used as the carrier gas at a flow-rate of 3 mL/min. The temperature gradient was as follows: initial 40°C for 5 min, ramped at 30°C/min to 240°C, and then held for 1 min. The mass spectrometer was operated in electron ionization mode with automatically tuned parameters, and the acquired mass range was m/z=15-200. The CO_2 signal was identified by the same retention time as the authentic sample prepared with dry-ice, and the production of $^{13}CO_2$ was compared by extracting m/z=45 (Fig. S3).

Anaerobic enzymatic assays. For anaerobic enzymatic assays, glucose oxidase and catalase powder (Sigma) were dissolved in 20 mM Tris (pH 8.5) in the anaerobic chamber to make stock solutions at 100 U/mL and 6,000 U/mL, respectively. 1 mL of reaction mixture contains 50 mM MES buffer (pH 6.2), 300 mM NaCl, 100 μM $(NH_4)_2Fe(SO_4)_2$, 1 mM ascorbic acid, 100 μM LA, 2 U/mL glucose oxidase, 120 U/mL catalase, 15 mM glucose, and 10 μM UndA. The reaction was initiated by adding UndA, incubated for 1 min, and quenched with 1 mL of 5 M NaOH in a sealed headspace vial (Fig. S4). The control group lacked glucose oxidase and was performed in the presence of ambient oxygen. SPME-GCMS detection of 1-undecene was performed as described as above.

Site-directed mutagenesis of undA. Glu_{101}, His_{104}, and His_{194} in UndA were all mutated to Ala using the QuikChange Site-Directed Mutagenesis Kit (Agilent) following the manufacturer's protocol and using primers pZR60_E101A_F/R, pZR60_H104A_F/R, and pZR60_H194A_F/R, respectively (Table S1). Mutations were verified by DNA sequencing.

Crystallography. Purified apo-UndA was incubated with 0.1 mM $(NH_4)_2Fe(SO_4)_2$ for 10 min, then buffer-exchanged into 10 mM Tris (pH 8.5), 100 mM NaCl, and 0.2 M $(NH_4)_2SO_4$ and concentrated to 10 mg/mL. UndA crystals were grown at room temperature using the hanging-drop vapor diffusion method in 0.1M MES, 1.8 M $(NH_4)_2SO_4$, 0.2 mM $(NH_4)_2Fe(SO_4)_2$, pH 6.5-7.0. To obtain ligand bound structures, UndA was incubated with 2.5 mM DEA or BHDA on ice for 15 min before crystallization. X-ray diffraction data were collected at beamline 8.3.1 at the Advanced Light Source (ALS) at Lawrence Berkeley National Laboratory. Diffraction data were integrated with MOSFLM (5) and scaled with SCALA (6). The initial phases were obtained by the molecular replacement method using search models of PSPTO1738 (PDB entry: 3OQL). The structure models were iteratively built with COOT (7) and refined with Phenix (8) and REFMAC5 (9). Resolution limits were determined using the $CC_{1/2}$ parameter, as defined by Karplus and Diederichs (10). Table S2 summarizes the statistics of data collection and refinement. The O-O bond lengths of the dioxygen species in 2,3-dodecenoic acid- and β-hydroxydodecanoic acid-bound proteins were refined without restraints on bond length. Simulated annealing omit maps were calculated with Phenix. All of the structural figures presented in this manuscript (Fig. 3 and Fig. S12) were prepared with the molecular visualization software PyMol (http://www.pymol.org).

Phylogenetic analysis. We search the homologs of PFL_4321 against the IMG/JGI database (https://img.jgi.doe.gov/cgi-bin/w/main.cgi) containing finished or permanent draft of sequenced genomes. 1676 total hits were acquired. MEGA 3.1 was applied for the sequence alignment and molecular evolutionary analysis of 1-undecene biosynthetic enzymes. The consensus phylogenetic tree was constructed using Neighbor-Joining method tested with Bootstrap with 1000 replications (Fig. S15).

1. Dassama LMK*, et al.* (2012) O-2-Evolving Chlorite Dismutase as a Tool for Studying O-2-Utilizing Enzymes. *Biochemistry-Us* 51(8):1607-1616.
2. Rui Z, Sandy M, Jung B, Zhang W (2013) Tandem enzymatic oxygenations in biosynthesis of epoxyquinone pharmacophore of manumycin-type metabolites. *Chem Biol* 20(7):879-887.
3. Ouchi A, Nakano M, Nagaoka S, Mukai K (2009) Kinetic study of the antioxidant activity of pyrroloquinolinequinol (PQQH(2), a reduced form of pyrroloquinolinequinone) in micellar solution. *J Agric Food Chem* 57(2):450-456.
4. Eser BE, Das D, Han J, Jones PR, Marsh EN (2011) Oxygen-independent alkane formation by non-heme iron-dependent cyanobacterial aldehyde decarbonylase: investigation of kinetics and requirement for an external electron donor. *Biochemistry-Us* 50(49):10743-10750.
5. Battye TG, Kontogiannis L, Johnson O, Powell HR, Leslie AG (2011) iMOSFLM: a new graphical interface for diffraction-image processing with MOSFLM. *Acta Crystallogr D Biol Crystallogr* 67(Pt 4):271-281.
6. Winn MD*, et al.* (2011) Overview of the CCP4 suite and current developments. *Acta Crystallogr D Biol Crystallogr* 67(Pt 4):235-242.
7. Emsley P, Cowtan K (2004) Coot: model-building tools for molecular graphics. *Acta Crystallogr D Biol Crystallogr* 60(Pt 12 Pt 1):2126-2132.
8. Adams PD*, et al.* (2002) PHENIX: building new software for automated crystallographic structure determination. *Acta Crystallogr D Biol Crystallogr* 58(Pt 11):1948-1954.
9. Murshudov G, Vagin A, Dodson E (1997) Refinement of macromolecular structures by the maximum-likelihood method. *Acta Crystallogr D Biol Crystallogr* 53(Pt 3):240-255.
10. Karplus PA, Diederichs K (2012) Linking crystallographic model and data quality. *Science* 336(6084):1030-1033.

Table S1. Primers used in this study

pZR60-F	GGTATTGAGGGTCGCATGATCGACACATTCAGCCG
pZR60-R	AGAGGAGAGTTAGAGCCTCAGCCTTCGGCCAGTGC
pZR60-F_HRV3C*	GGTATTGAGGGTCGCCTTGAAGTCCTCTTTCAGGGACCCATG ATCGACACATTCAGCCG
pZR60_E101A_F	GCAATATCCGGGTCGCGCTCAATCATGCCGA
pZR60_E101A_R	TCGGCATGATTGAGCGCGACCCGGATATTGC
pZR60_H104A_F	CAGTAATCGGCAGCATTGAGCTCGACCCGGATATTGC
pZR60_H104A_R	GCAATATCCGGGTCGAGCTCAATGCTGCCGATTACTG
pZR60_H194A_F	GAAGTGGCTGAAGATGGCTGCCCAGTACGACGAC
pZR60_H194A_R	GTCGTCGTACTGGGCAGCCATCTTCAGCCACTTC
pZR80_F	GGTATTGAGGGTCGCATGATCGACACTTTCGAGAG
pZR80 R	AGAGGAGAGTTAGAGCCCTACATTTCCAGTGCGGC
pZR95_F	GGTATTGAGGGTCGCA TGAGCGAGTTCTTTGACCG
pZR95_R	AGAGGAGAGTTAGAGCC CTACTCCGCGCCGACCGC
pZR97_F	GGTATTGAGGGTCGCA TGGAAATCACAAGGATCAA
pZR97_R	AGAGGAGAGTTAGAGCC TCAGCCCGCAGCCAACGC

*the human rhinovirus 3C proteinase site is underlined

Table S2. Data collection and refinement statistics

	Holo	DEA-bound	BHDA-bound
Data collection			
Space group	C222 (21)	P2221 (17)	P2221 (17)
Cell dimensions			
a, *b*, *c* (Å)	141.38, 218.44, 67.31	67.48, 74.16, 142.50	67.41, 73.99, 142.51
α, β, γ (°)	90.00, 90.00, 90.00	90.00, 90.00, 90.00	90.00, 90.00, 90.00
Resolution (Å)	58.55-1.90 (1.94-1.90)*	71.25-1.80 (1.84-1.80)	73.99-1.70 (1.73-1.70)
CC(1/2)	0.995 (0.169)	0.996 (0.205)	0.999 (0.425)
R_{merge}	0.12 (1.63)	0.17 (2.28)	0.085 (1.256)
I / σ	9.7 (1.7)	8.1 (0.6)	14.5 (1.1)
Completeness (%)	99.9 (99.9)	97.0 (94.9)	95.8 (70.9)
Redundancy	4.4 (4.3)	6.7 (4.9)	8.4 (5.1)
Refinement			
Resolution (Å)	54.67-1.90 (1.97-1.90)	71.35-1.8 (1.86-1.80)	65.75-1.70 (1.76-1.70)
No. reflections	72,082 (8,157)	63,640 (6,049)	75,678 (5662)
R_{work} / R_{free}	0.143/0.194 (0.315/0.357)	0.161/0.229 (0.321/0.368)	0.137/0.185 (0.306/0.301)
No. atoms			
Protein	4201	4170	4182
Ligand/ion	95	90	76
Iron ion	2	2	2
Water	558	497	564
B-factors			
Protein	34.40	33.70	29.90
Ligand/ion	55.30	60.90	52.30
Iron ion	26.57	30.15	26.46
Water	46.60	43.60	42.70
R.m.s. deviations			
Bond lengths (Å)	0.021	0.011	0.011
Bond angles (°)	2.00	1.33	1.30
Ramachandran			
Favored (%)	98	98	99
Allowed (%)	2	2	2
Outlier (%)	0	0	0

*Values in parentheses are for the highest-resolution shell.

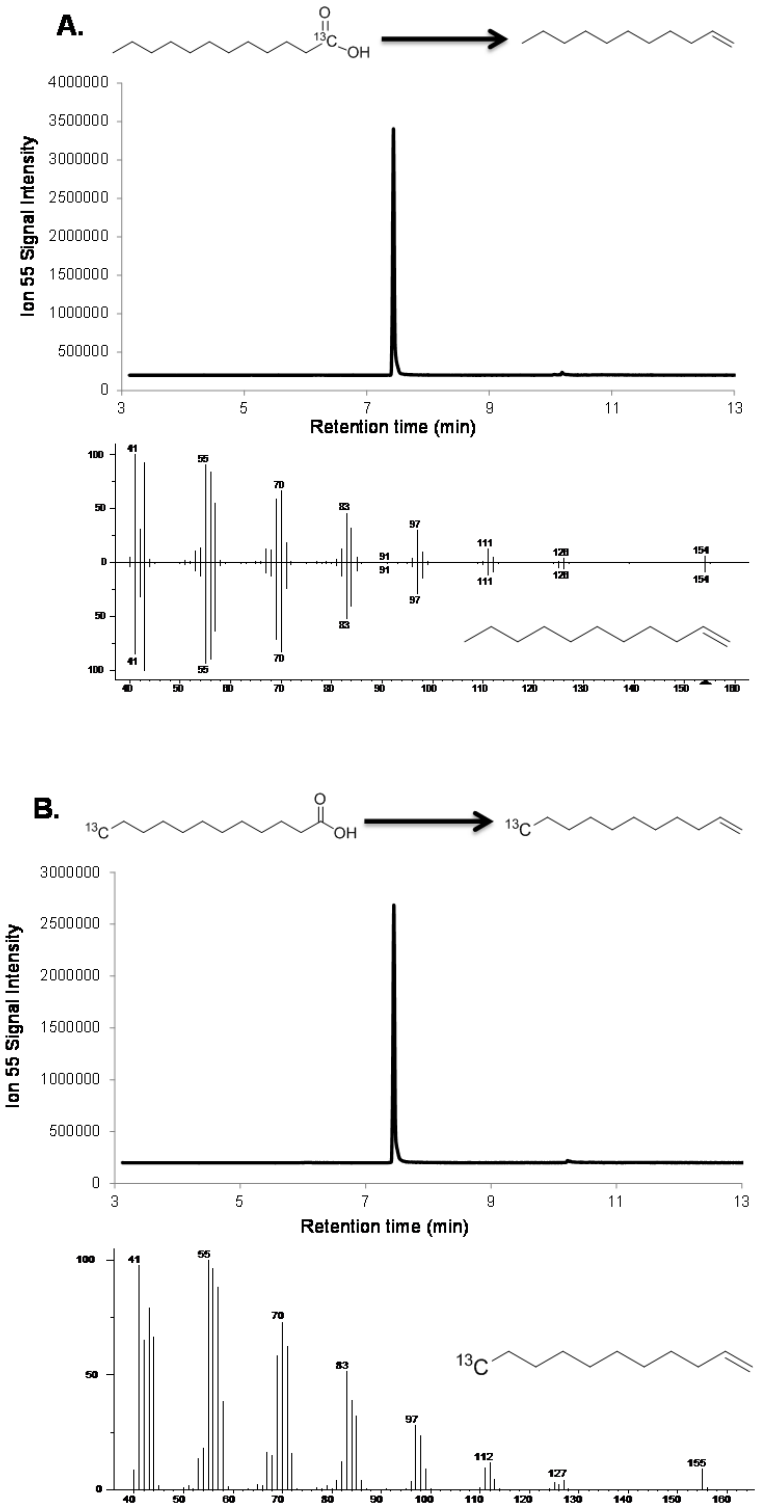

Figure S1. GC-MS analysis of the conversion of [12-^{13}C]lauric acid and [1-^{13}C]lauric acid to [11-^{13}C]undecene (**B**) and [U-^{12}C11]undecene (**A**), respectively. Reverse panel in (**A**) shows the reference standard of 1-undecene from the NIST spectral database.

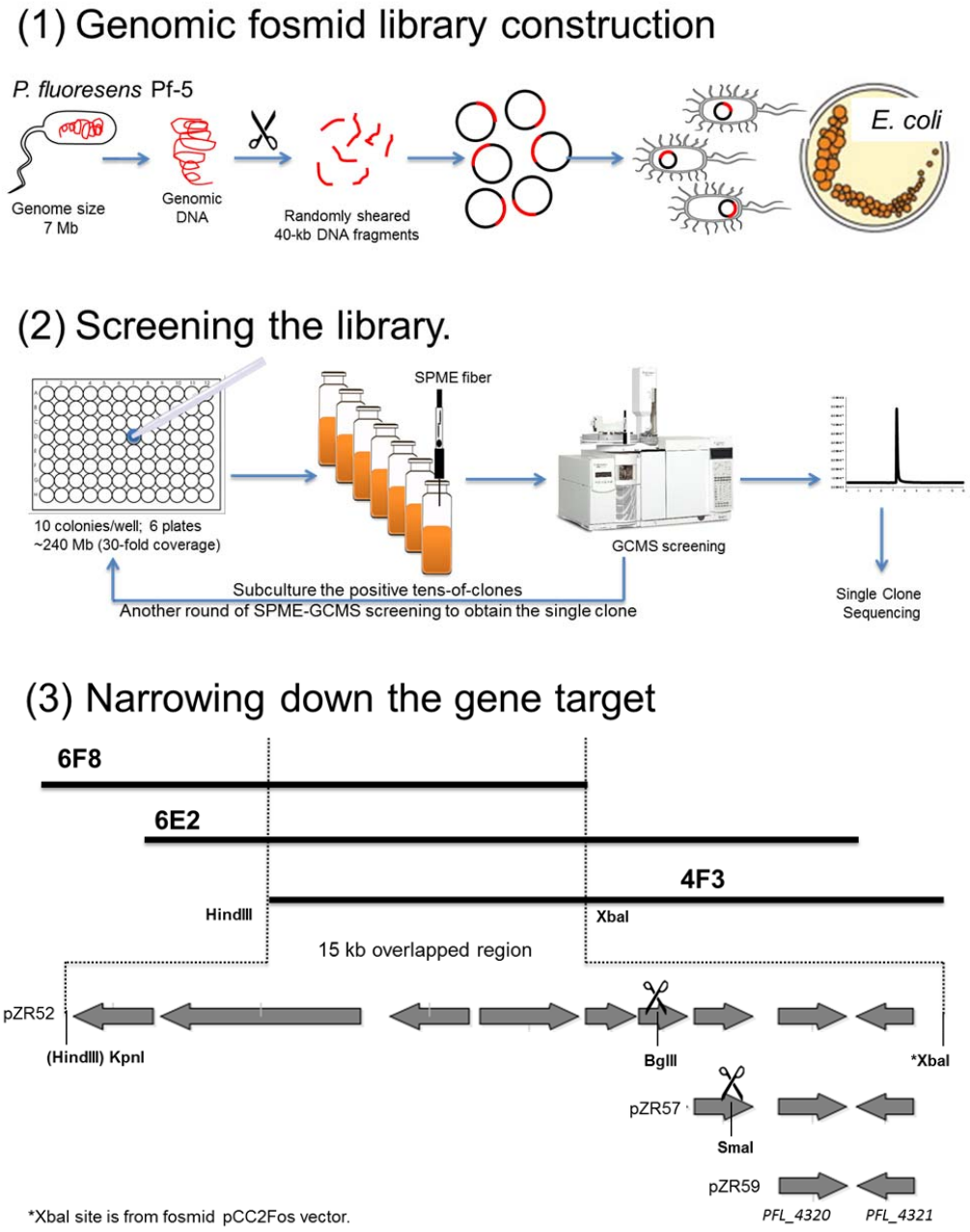

Figure S2. Flow chart for the identification of 1-undecene biosynthetic gene by heterologous expression of the genomic library of *P. fluoresens* Pf-5. From the library screening, three positive fosmid clones, 6F8/6E2/4F3, were identified to be responsible for 1-undecene production in *E. coli*. The 15 kb overlapping region was further trimmed by restriction digestion and narrowed down to two genes, *PFL_4320* and *PFL_4321 (undA)*. When *PFL_4320* and *undA* were separately overexpressed in *E. coli* BL21, only *undA* conferred 1-undecene production.

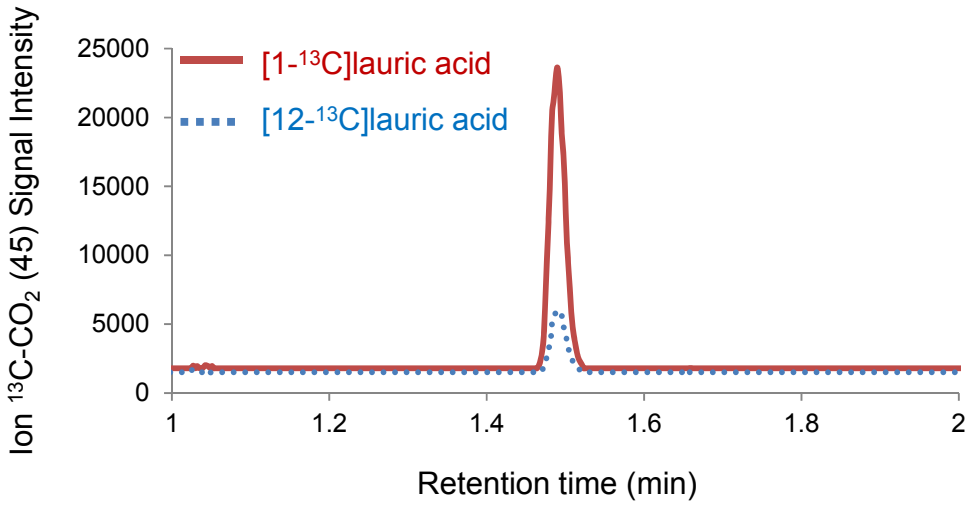

Figure S3. GC-MS detection of ^{13}C-CO$_2$ formation by UndA activity. [12-^{13}C]lauric acid was used as a negative control to show the natural abundance of ^{13}C-CO$_2$.

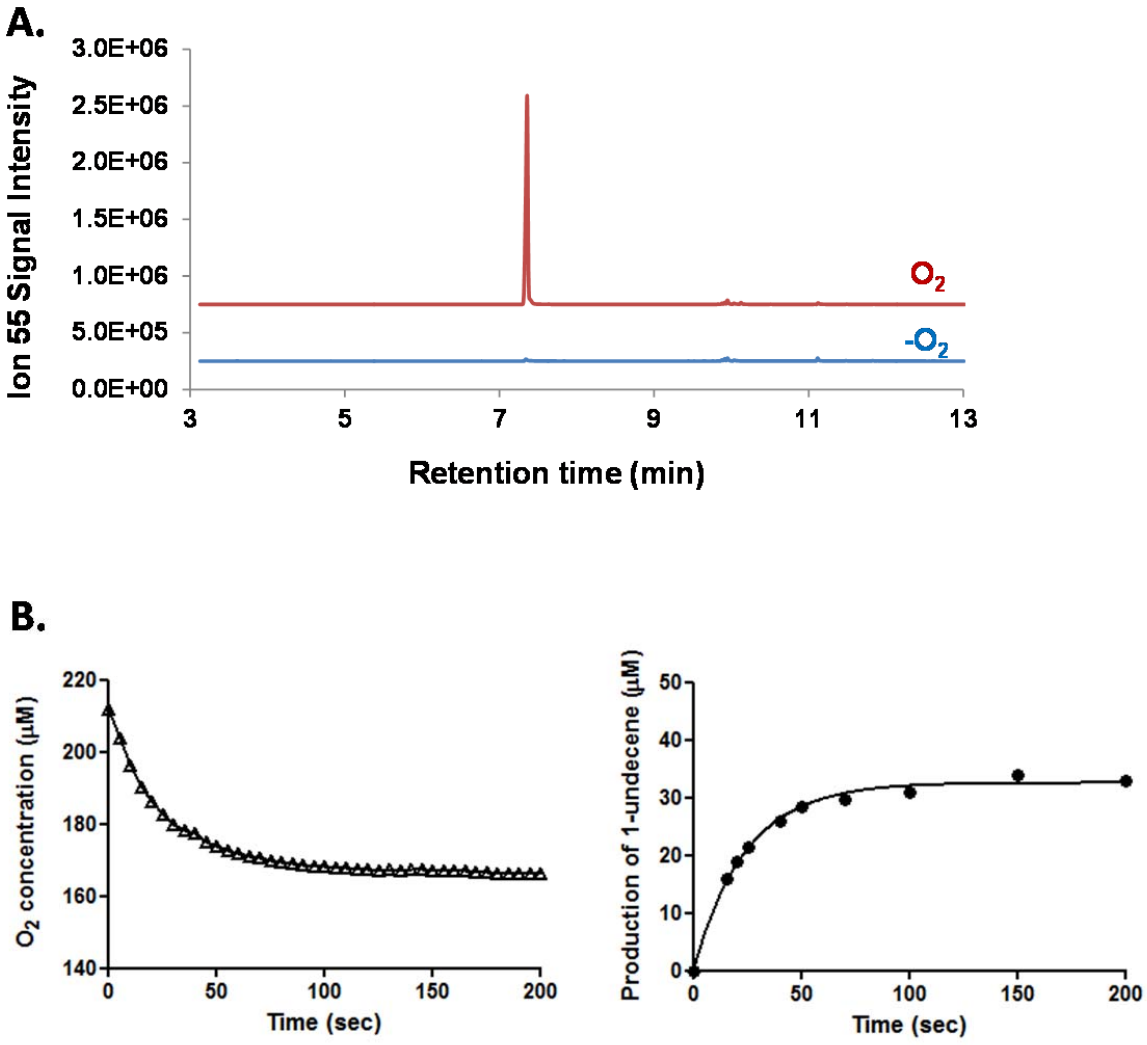

Figure S4. Requirement of O_2 for UndA activity. Panel (**A**) shows GC-MS detection of 1-undecene production by UndA in the aerobic/anaerobic assays. The anaerobic assay was performed by using the anaerobically purified enzyme and degassed reagents, adding glucose oxidase/glucose/catalase, and conducting the experiment in an anaerobic chamber with ppm O_2 < 0.7. The control aerobic assay was performed by using a similar reaction mixture under ambient air conditions and omitting glucose oxidase. Panel (**B**) shows the consumption of dissolved oxygen detected by the oxygen electrode in relation with the formation of 1-undecene measured by SPME-GCMS in a typical reaction mixture containing 50 mM MES buffer (pH 6.2), 300 mM NaCl, 45 µM holo-UndA, and 500 µM LA.

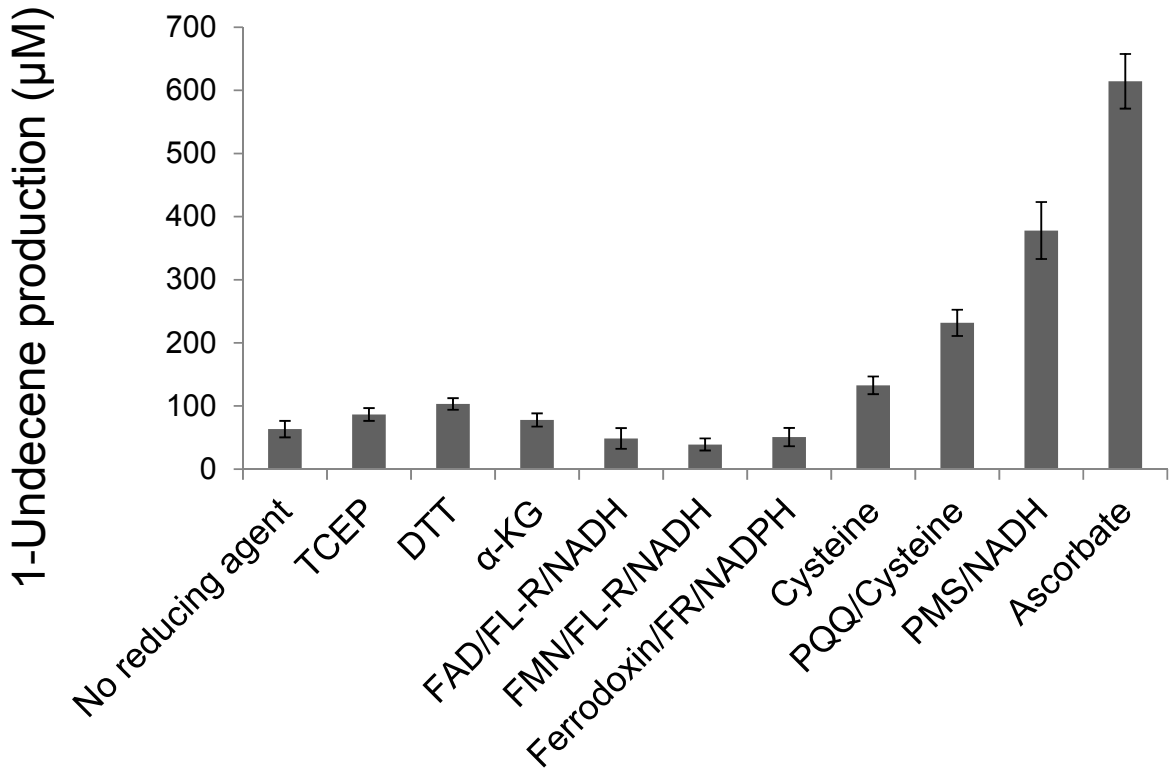

Figure S5. Comparison of 1-undecene production by using various reductive cofactors/co-substrates in the presence of excess O_2 provided by the coupled chloride dismutase reaction. The reaction mixture contains 100 μM MES (pH 6.1), 300 mM NaCl, 1 mM lauric acid (dissolved in 0.5% tergitol), 100 μM UndA, 100 μM $(NH_4)_2Fe(SO_4)_2$, 2 μM chlorite dismutase, 4 mM sodium chlorite, and 2 mM reductive cofactor/co-substrates. When needed, 40 μM FAD, FMN, ferredoxin, PQQ, or PMS, and 20 μM flavin reductase (FL-R) or ferredoxin reductase (FR) were added. 1-Undecene production was analyzed after reacting for 100 min. Error bars represent standard deviations from at least three independently performed experiments.

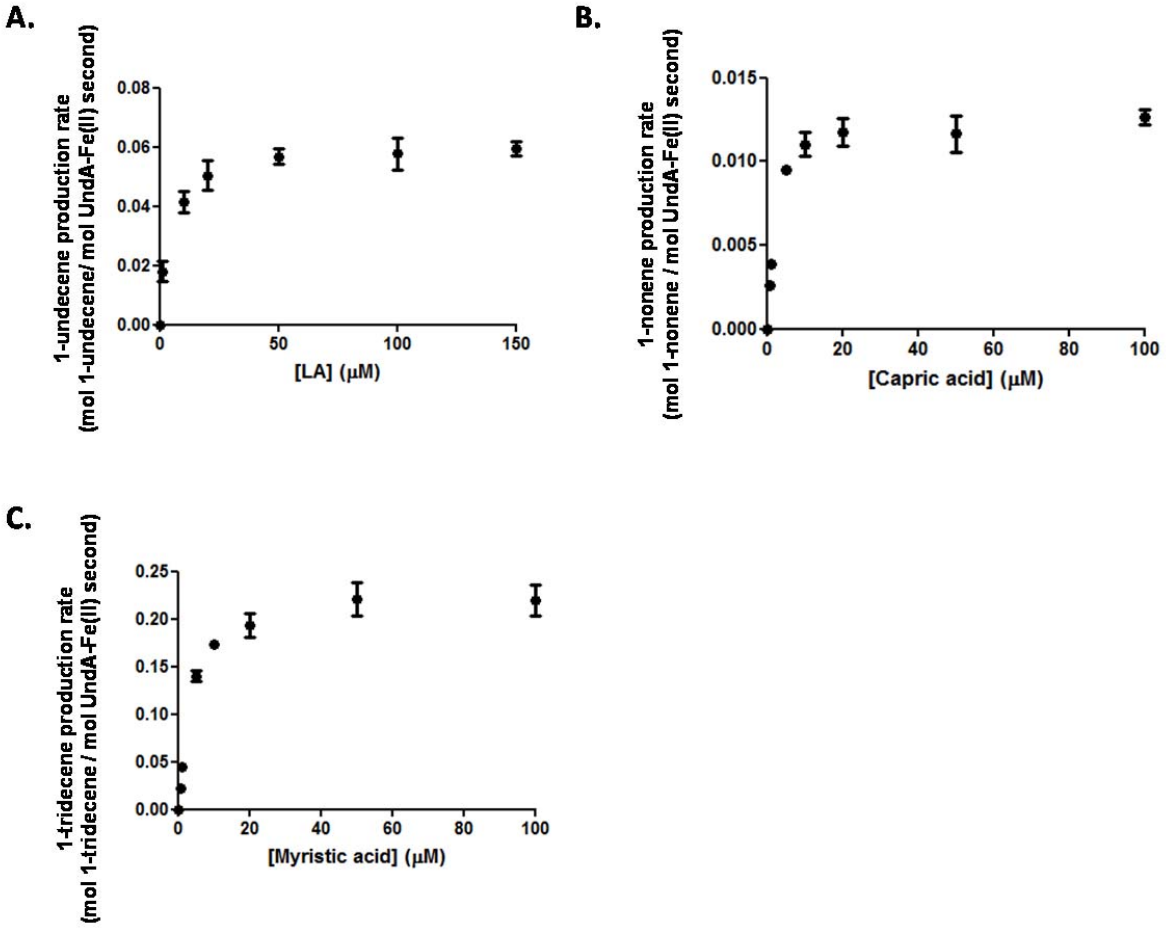

Figure S6. Measured initial production rates of 1-alkenes by UndA at varying substrate concentrations. Error bars represent standard deviations from at least three independently performed experiments.

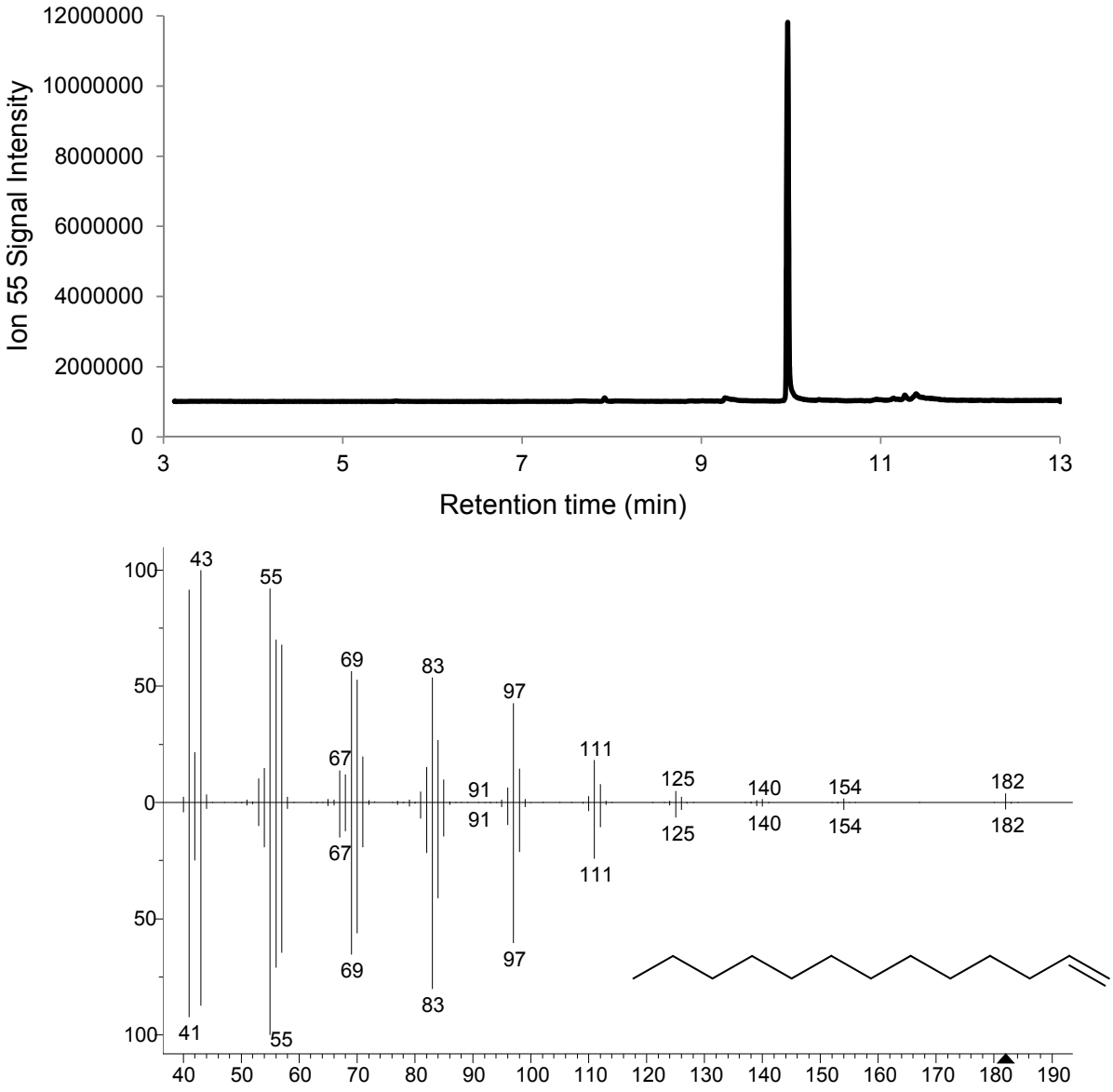

Figure S7. GC-MS analysis of the conversion of myristic acid to 1-tridecene. Reverse panel shows the reference standard of 1-tridecene from the NIST spectral database.

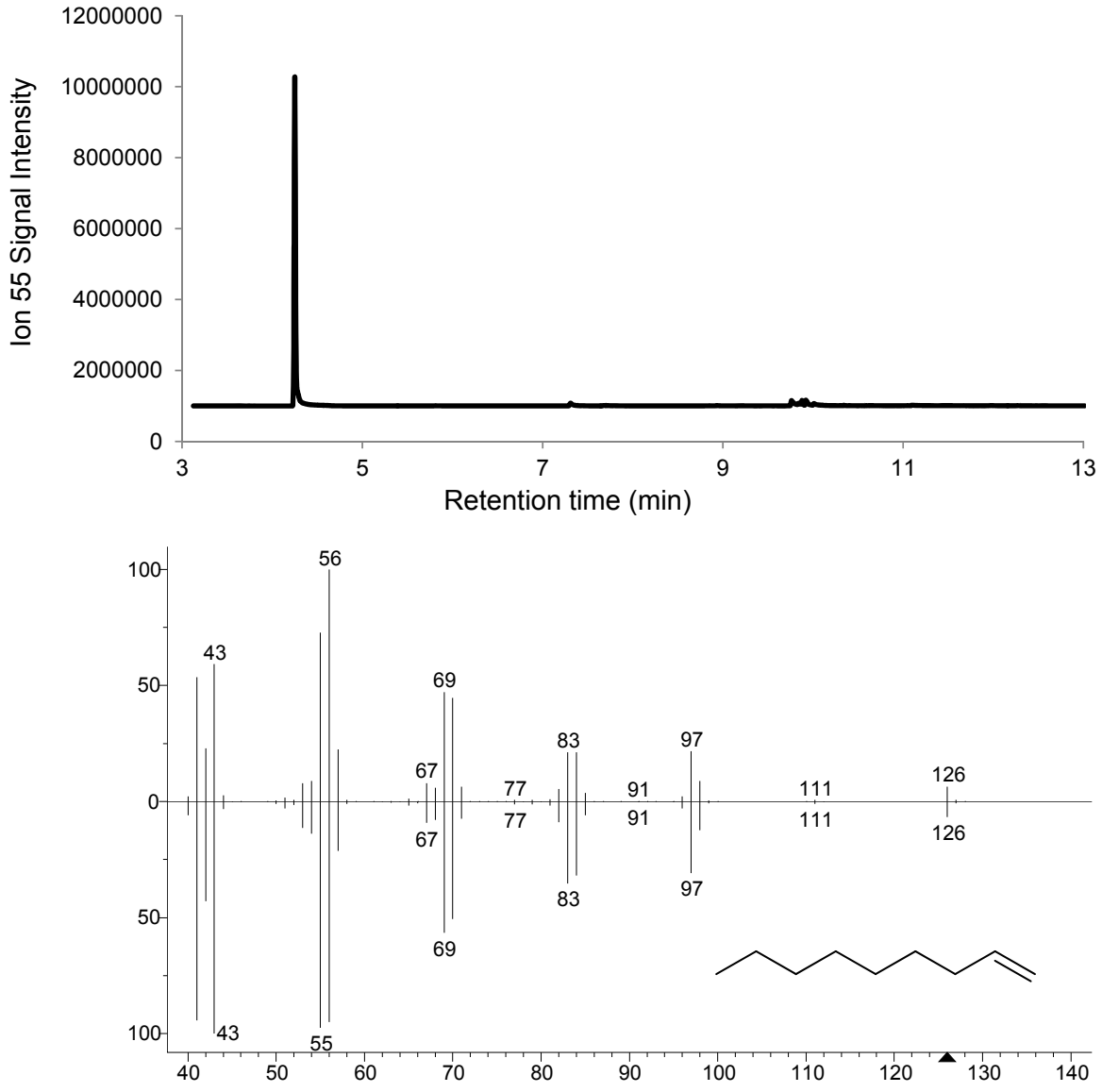

Figure S8. GC-MS analysis of the conversion of capric acid to 1-nonene. Reverse panel shows the reference standard of 1-nonene from the NIST spectral database.

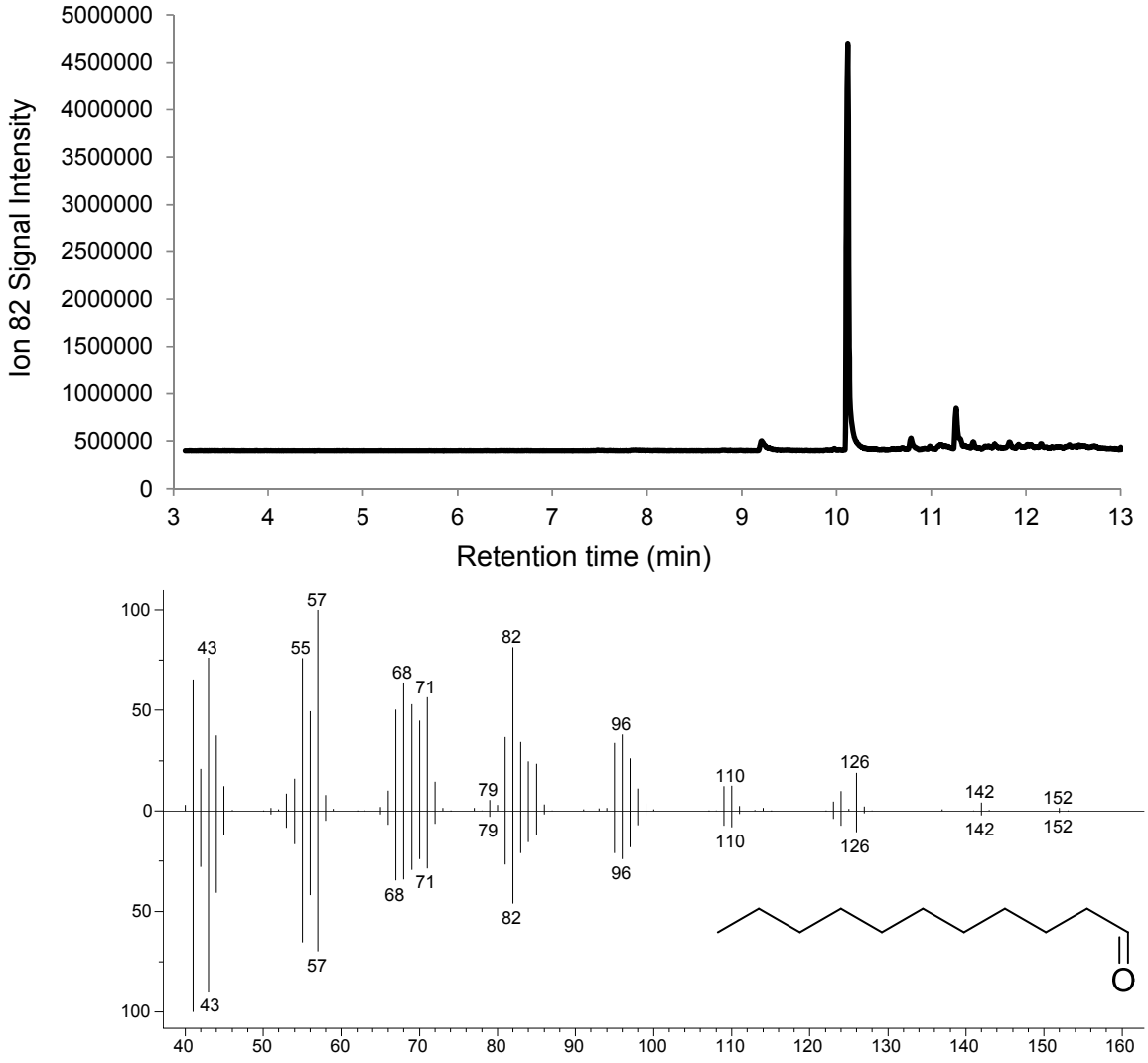

Figure S9. GC-MS analysis of the conversion of α-hydroxydodecanoic acid (AHDA) to 1-undecanal. Reverse panel shows the reference standard of 1-undecanal from the NIST spectral database.

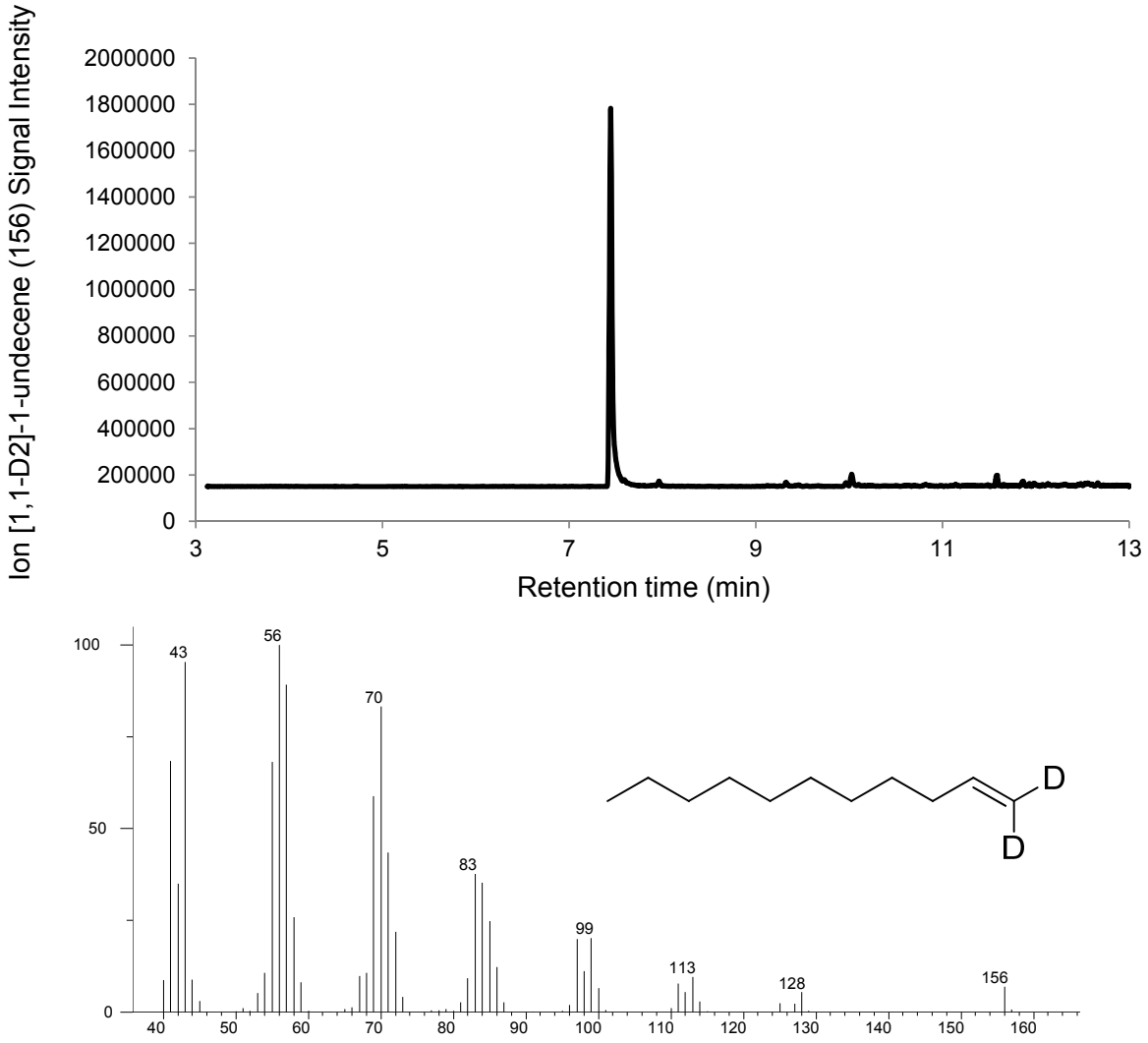

Figure S10. GC-MS analysis of the conversion of [2,2-D2]lauric acid to [1,1-D2]undecene. The both deuterium atoms of [α,α-D2]lauric acid are proposed to retain at the α-carbon position.

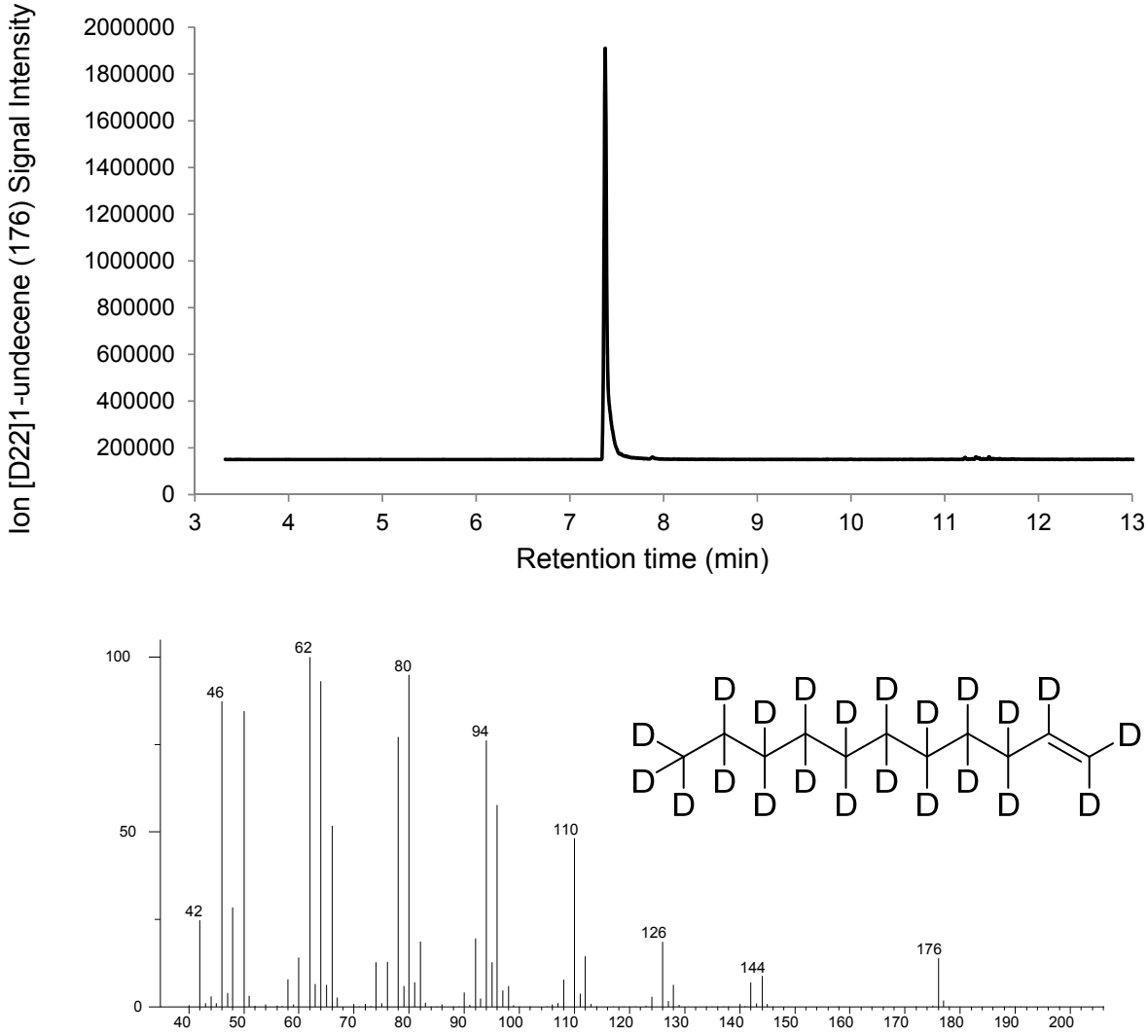

Figure S11. GC-MS analysis of the conversion of [D23]lauric acid to [D22]1-undecene.

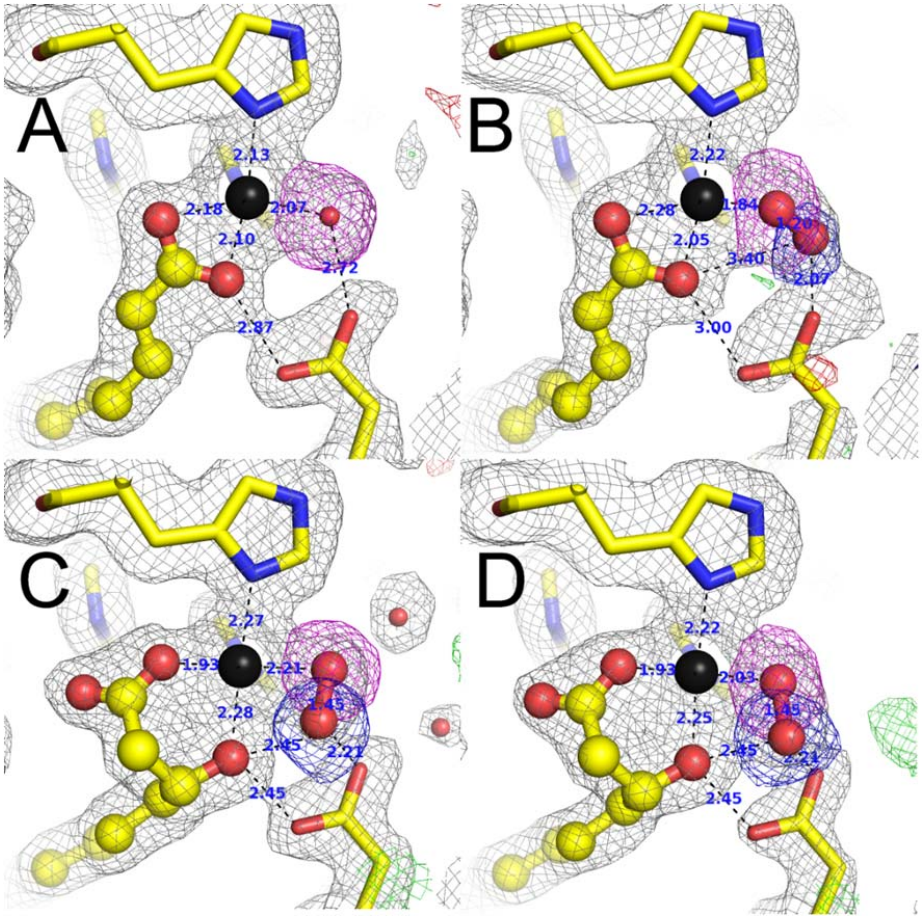

Figure S12. Geometry of the active sites. Weighted electron density maps surrounding the active site of the UndA/DEA complex (chain A (**A**) and chain B (**B**)) and the active site of the UndA/BHDA complex (chain A (**C**) and chain B (**D**)) with 2mF_O-DF_C (in gray, contoured at 1.0 σ). The simulated annealing electron density maps after omitting the proximal O1 atom are colored in magenta; and after omitting the distal O2 atom are colored in blue. All omit maps are contoured at 4.0 σ. The orientation is approximately equivalent to that shown in the schematic in Fig. 3f.

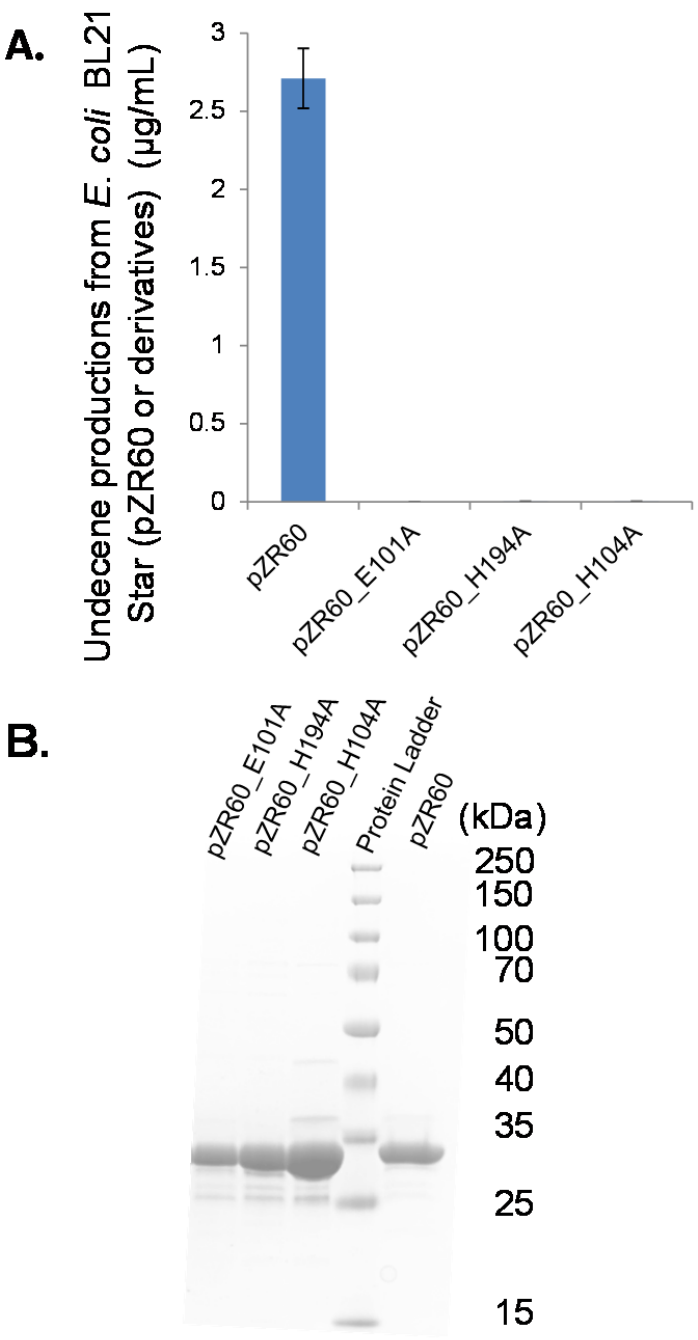

Figure S13. Comparison of 1-undecene production by *E. coli* BL21 (pZR60) and *E. coli* BL21 (pZR60 derivatives bearing point mutations on *undA*). Error bars represent standard deviations from at least three independently performed experiments. Panel (**B**) shows that the mutated proteins are soluble.

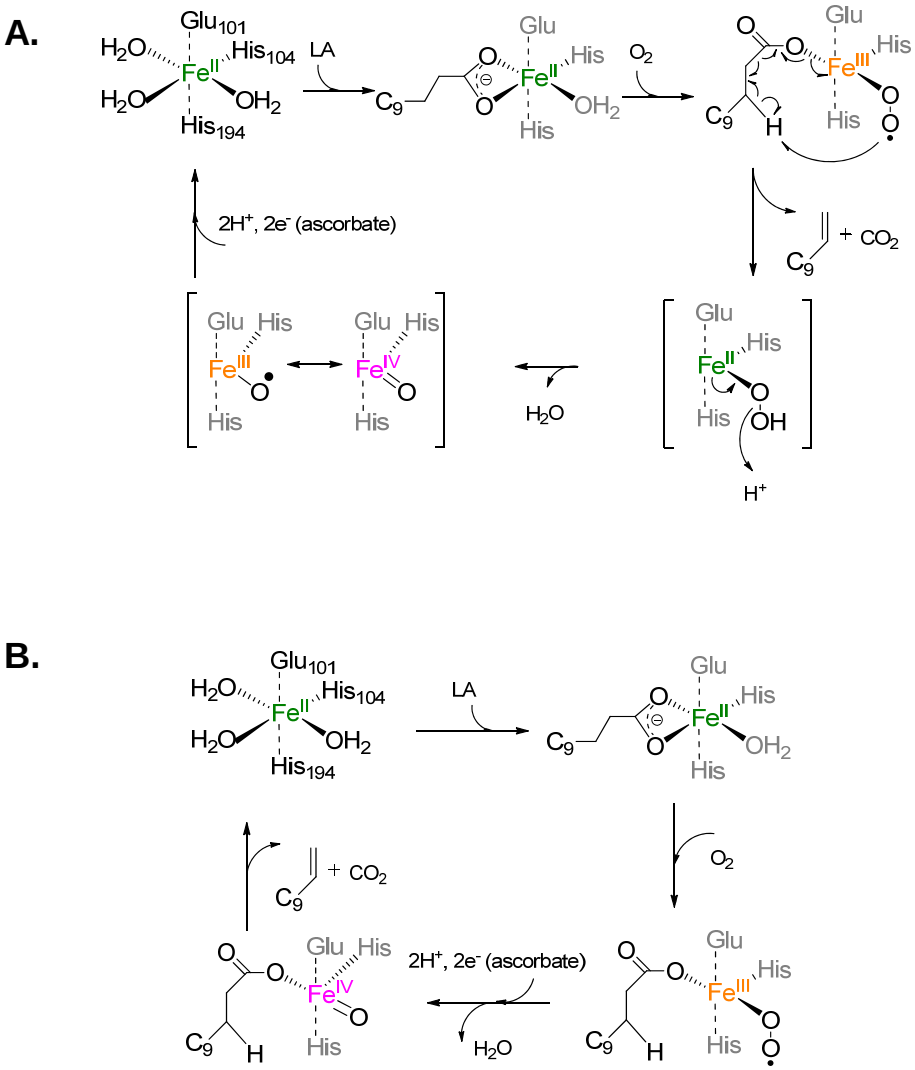

Figure S14. Possible mechanisms for the UndA reaction.

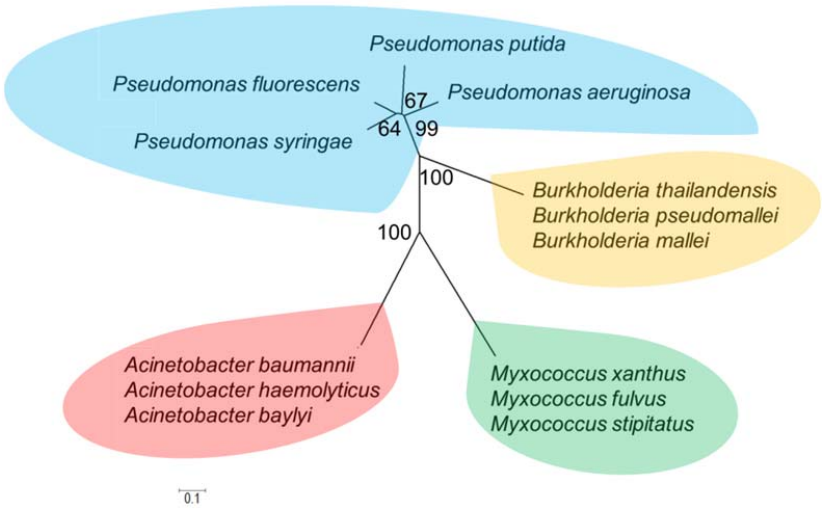

Figure S15. Phylogenetic tree of UndA and homologs constructed using Neighbor-Joining method. The UndA homologs in *Burkholderia* are in the similar operon as in *Pseudomonas*, but the ones in *Acinetobacter* and *Myxococcus* are organized in different operons.